

Resonant current from singlet-triplet state mixing in coupled quantum dots

G. Giavaras*

Electrically driven spin resonances in double quantum dots can lift the spin blockade and give rise to a resonant current. This current can probe the properties of coupled two-spin states for different quantum dot configurations. Using a Floquet-Markov quantum transport model we compute the resonant current for different driving amplitudes and ac field frequencies in spin-orbit coupled quantum dots. We show that the resonant current has a very rich interference pattern which can give valuable insight into the singlet-triplet state mixing.

Introduction– Spins in semiconductor quantum dots can be controlled electrically and are promising not only for quantum-gate engineering [1] but also for studying correlation effects, decoherence, and transport properties in the nanoscale [2–30]. In a double quantum dot (DQD) in the spin-blockade regime [31] the singlet energy levels define a two-level system with an anticrossing point that is the result of coherent interdot tunneling. When an ac electric field is added to the DQD [32] this anticrossing allows for Landau-Zener-Stückleberg-Majorana (LZSM) transitions and interference [33–36]. Such transitions have been studied in detail not only in semiconducting [33–36] but also in various superconducting quantum systems [35, 36]. Furthermore, hybridized singlet-triplet states in tunnel-coupled quantum dots can serve as qubits which can be probed with microwave fields and electrical transport measurements [1–4, 28, 37–39]. Then, some of the coherence properties of the qubit can be extracted from the resonant current flowing through the DQD.

For the appropriate driving amplitude the current can map out the two-spin energy levels [4, 28–30, 37] and the singlet-triplet anticrossing. Depending on the energy configuration of the DQD the ac field can induce different types of transitions. Some typical cases include, for example, transitions between the two energy levels forming the anticrossing or transitions between a third energy level and the two levels that anticross. In both cases the ac field induced resonant current has been measured revealing the singlet-triplet anticrossing [4, 37]. Here, we show that beyond the spectroscopic regime which focuses on the anticrossing gap, the resonant current can exhibit a rich interference pattern. This can be very sensitive to the exact driving frequency and the resonant region can undergo a drastic change. Exploring the current within a narrow energy detuning range and different ac field frequencies gives insight into a singlet-triplet state mixing.

AC-induced resonant current– In the present work we consider two tunnel-coupled quantum dots in the spin blockade regime [31]. The quantum dots are coupled to metallic leads, so when the spin blockade is lifted electrical current can flow through the DQD. The physical system is described using the same quantum transport model as in Ref. 29. We assume that an ac electric field modulates periodically the energy detuning of the DQD,

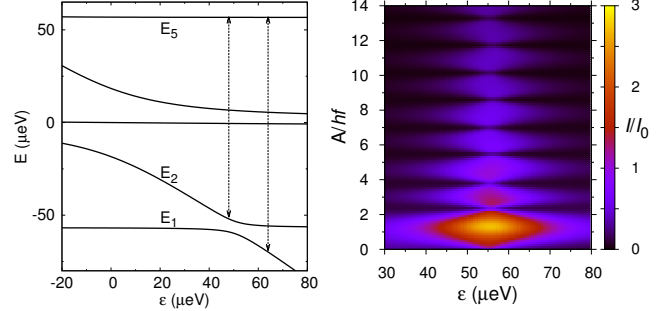


FIG. 1. Left frame: Energy levels of double quantum dot as a function of energy detuning at $B = 0.135$ T with $t_c = 13$ μeV , $t_{\text{so}} = 3.5$ μeV , $g_1 = 7$, and $g_2 = 7.5$. Typical frequencies considered in this work are indicated by vertical arrows. Right frame: Resonant current as a function of ac field amplitude and energy detuning at $f = 27$ GHz with $I_0 \approx 1$ pA.

namely,

$$\delta(t) = -\varepsilon + A \cos(2\pi ft). \quad (1)$$

Without the driving field ($A = 0$) the time independent parameter ε controls the character of the singlet states as well as the singlet-triplet spacing. When $A \neq 0$ and for the appropriate frequencies electrically driven spin-resonances can be induced and a resonant current flows through the DQD. For large driving amplitudes LZSM dynamics becomes relevant resulting in interference fringes [35, 36]. The DQD Hamiltonian in the singlet-triplet basis: $|S_{11}\rangle$, $|T_+\rangle$, $|S_{02}\rangle$, $|T_-\rangle$, and $|T_0\rangle$ is given in matrix form [29]

$$H = \begin{pmatrix} 0 & 0 & -\sqrt{2}t_c & 0 & \Delta^- \\ 0 & -\Delta^+ & -t_{\text{so}} & 0 & 0 \\ -\sqrt{2}t_c & -t_{\text{so}} & \delta & -t_{\text{so}} & 0 \\ 0 & 0 & -t_{\text{so}} & \Delta^+ & 0 \\ \Delta^- & 0 & 0 & 0 & 0 \end{pmatrix}, \quad (2)$$

with the time dependent detuning, $\delta = \delta(t)$, and the Zeeman splitting terms $\Delta^\pm = (\Delta_2 \pm \Delta_1)/2$, $\Delta_i = g_i \mu_B B$.

In the spin blockade regime the two lowest singlet states of the DQD form an anticrossing point for $\varepsilon = 0$ due to coherent interdot tunneling ($t_c \neq 0$). In this tunneling process the spin is conserved. Tuning ε changes the character of the singlet states from $(1, 1)$ to $(0, 2)$ where the notation (n, m) indicates n (m) electrons in the left (right) quantum dot. In addition, the two lowest

* Quantum Laboratory Kivotos, g.giavaras@gmail.com

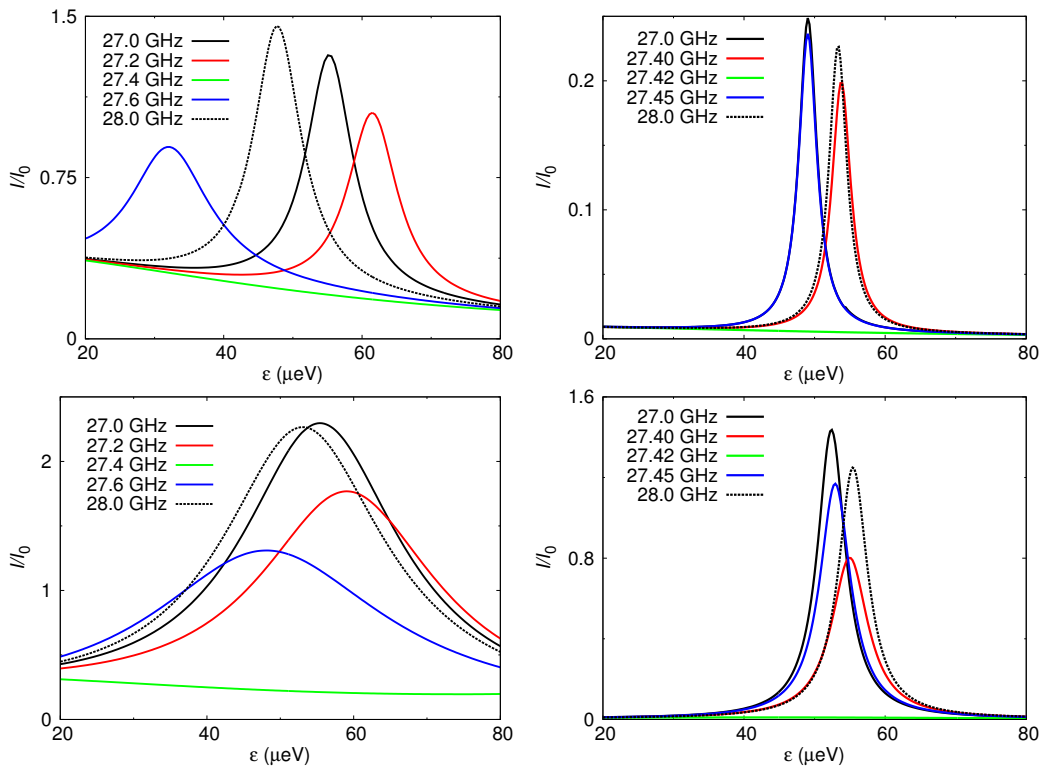


FIG. 2. Resonant current as a function of energy detuning at different ac field frequencies with $t_{so} = 3.5 \mu\text{eV}$ (left), and $t_{so} = 0.5 \mu\text{eV}$ (right). Upper frames: $A = 20 \mu\text{eV}$. Lower frames: $A = 100 \mu\text{eV}$.

singlet states and the $S_z = \pm 1$ triplet states form anti-crossing points due to a nonzero spin-orbit tunneling coupling ($t_{so} \neq 0$). This tunneling involves a coherent spin flip forming hybridized singlet-triplet states. For such a DQD system an earlier work [29] has explored the ac-induced current as a function of the driving amplitude and demonstrated the significant role of t_{so} in the interference profile. Most importantly ac-induced blocked (dark) states suppress the resonant current at very characteristic values of the ratio A/hf [29]. Despite the fact that Ref. 29 focuses on a narrow energy detuning range for $\varepsilon > 0$, the results can be straightforwardly extended to larger positive detunings as well as to $\varepsilon \leq 0$. In this case interference fringes can be observed which resemble those of a two-level quantum system.

The eigenenergies ($A = 0$) of the DQD as a function of the detuning are plotted in Fig. 1. At $\varepsilon \approx 50 \text{ meV}$ the energy level E_5 corresponds to a triplet-like state, whereas the levels E_1 and E_2 correspond to hybridised singlet-triplet states due to $t_{so} \neq 0$. In the present work typical frequencies are of the order of $hf \sim E_5 - E_1 \approx E_5 - E_2$ and the resonant current is computed for small values of ε near zero. Larger positive detunings as well as negative values can equally be considered. The resonant current is obtained from the steady-state density matrix of the DQD. This density matrix obeys a Floquet-Markov master equation of motion [40] in the sequential tunneling regime and with the same periodicity as that of the ac field. This approach is more appropriate in order to cap-

ture strong driving effects, however, approximate treatments can provide valuable insight [28–30] even in the ‘multi-photon’ regime.

Some characteristic examples of the resonant current as a function of the energy detuning are shown in Fig. 2. Similar to an earlier study [29] we choose the ac field frequency to be of the order of $hf \sim E_5 - E_1 \approx E_5 - E_2$; this means that we tune the frequency so that to capture the anticrossing point between the levels E_1 and E_2 shown in Fig. 1. To clarify the role of the driving amplitude we compute the current for two different cases. When A is chosen to be relatively small, i.e., $A \approx 20 \mu\text{eV}$, the induced current peaks are indicative of singlet-triplet transitions which lift the spin blockade. However, increasing the driving amplitude gradually introduces deviations from this simple picture. This can be seen for $A \approx 100 \mu\text{eV}$ where the current peaks start to overlap. According to Fig. 2, small changes in f near the anticrossing lead to a noticeable current suppression; in agreement with an earlier work [29]. Specifically, the current peak is nearly vanished and the observed current is approximately equal to the current flowing through the DQD without the ac field ($A = 0$). This current is computed with the same model as in Ref. 23 and is always nonzero due to the inclusion of the single electron states in the equation of motion of the DQD density matrix. These lead to non-zero matrix elements between states differing by one electron, thus, lifting the ideal spin blockade condition [23].

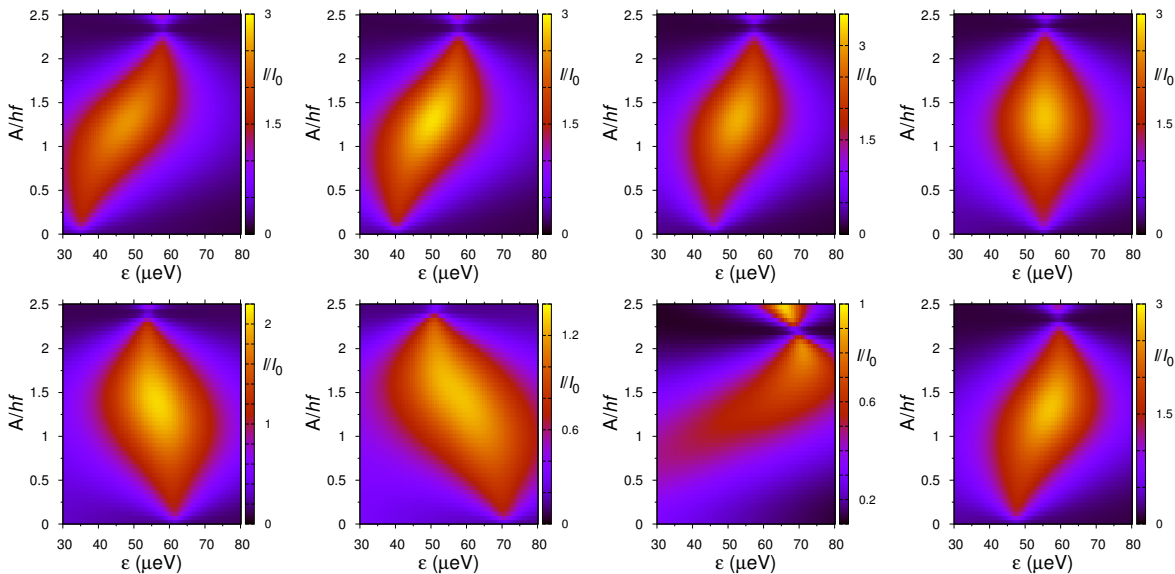


FIG. 3. Resonant current as a function of ac field amplitude and energy detuning for $t_{\text{so}} = 3.5 \mu\text{eV}$. The ac field frequency in GHz is: $f = 24, 25, 26, 27$ (upper frames) and $27.2, 27.3, 27.5, 28$ (lower frames).

A simple investigation shows that the current suppression in Fig. 2 marks the singlet-triplet anticrossing. Consequently, a smaller spin-orbit tunnel coupling (leading to a smaller anticrossing gap) requires a finer f -tuning for the current suppression to be observable. This remark is consistent with the results in Fig. 2 that correspond to $B = 0.135$ T. Decreasing the magnetic field gradually changes the character of the two-spin states, therefore deviations from the physical picture presented in Fig. 2 are expected especially at very low magnetic fields. In contrast, similar trends are observed at higher fields.

The results in Fig. 2 can be extended to larger values of A allowing us to go beyond the simple spectroscopic regime. An important aspect that complements the findings of an earlier work [29] is that the resonant current exhibits an interesting interference profile even for a (relatively) small amplitude to frequency ratio, i.e., $A/hf < 3$. To quantify this argument we present some results in Fig. 3 for different values of f . These reveal a high-current region that has similar characteristics to the region that has been predicted in an earlier study [29]. Increasing f leads to small changes in the resonant current, however, as f approaches the singlet-triplet anticrossing [$hf \approx (g_1 + g_2)\mu_B B$] the overall current profile becomes very sensitive to the exact value of f . Simultaneously a current suppression is observed, especially for small ratios A/hf , and a drastic change occurs in the resonant

region.

Although in Fig. 3 we focus on $\varepsilon > 0$ and near zero only, the above current characteristics can also be found for negative values of ε . In addition, increasing the ratio A/hf allows us to explore in more detail the resulting interference fringes (similar to Fig. 1) due to the LZMS dynamics. Finally, we remark that using a time dependent gate voltage to periodically control the energy detuning [Eq. (1)] is very likely to unintentionally induce a weak time dependence in the interdot tunnel coupling, t_c and/or t_{so} . This is probable to occur for large driving amplitudes, so for this reason a study of a realistic DQD should account for a weak time dependent tunnel coupling term. Theoretical studies [28, 30] have demonstrated that such a term gives rise to a resonant current that can dominate over the current in Fig. 3.

Summary– In summary, we computed the resonant current in tunnel coupled quantum dots for different ratios A/hf and energy detunings. We found that beyond the spectroscopic regime which reveals the anticrossing gap the resonant current exhibits a rich interference pattern. We showed that by considering a narrow detuning range and investigating the current at different ac field frequencies can give insight into a singlet-triplet state mixing. Our results can be validated with electrical transport measurements.

-
- [1] M. De Michielis, E. Ferraro, E. Prati, L. Hutin, B. Bertrand, E. Charbon, D. J. Ibberson, and M. F. G. Zalba, *J. Phys. D: Appl. Phys.* **56**, 363001 (2023).
 [2] J. R. Petta, A. C. Johnson, J. M. Taylor, E. A. Laird, A.

- Yacoby, M. D. Lukin, C. M. Marcus, M. P. Hanson, and A. C. Gossard, *Science* **309**, 2180 (2005).
 [3] J. M. Elzerman, R. Hanson, L. H. Willems van Beveren, B. Witkamp, L. M. K. Vandersypen, and L. P. Kouwen-

- hoven, *Nature* **430**, 431 (2004).
- [4] K. Ono, G. Giavaras, T. Tanamoto, T. Ohguro, X. Hu, and F. Nori, *Phys. Rev. Lett.* **119**, 156802 (2017).
- [5] J. S. Mollejo, D. Jirovec, Y. Schell, J. Kukucka, S. Calcaterra, D. Chrastina, G. Isella, M. R. Russ, S. Bosco, and G. Katsaros, arXiv:2408.03224
- [6] H. A. Abdulkhalaq, N. R. Abdullah, and V. Gudmundsson, *Physica E* **144**, 115405 (2022).
- [7] J. Xu, S. Wang, J. Wu, Y. Yan, J. Hu, G. Engelhardt, and J. Y. Luo, *Phys. Rev. B* **107**, 125113 (2023).
- [8] A. Sala and J. Danon, *Phys. Rev. B* **104**, 085421 (2021).
- [9] G. Giavaras, J. H. Jefferson, M. Fearn, and C. J. Lambert, *Phys. Rev. B* **75**, 085302 (2007).
- [10] M. P. Nowak and B. Szafran, *Phys. Rev. B* **89**, 205412 (2014).
- [11] H. B. Xue, X. Y. Ma, B. Chen, J. B. Chen, and L. L. Xing, *Physica E* **167**, 116159 (2025).
- [12] Z. Zhou, Y. Li, Z. Wu, X. Ma, S. Fan, and S. Huang, *J. Semicond.* **45**, 101701 (2024).
- [13] G. Giavaras, J. H. Jefferson, M. Fearn, and C. J. Lambert, *Phys. Rev. B* **76**, 245328 (2007).
- [14] G. Giavaras and F. Nori, *Phys. Rev. B* **94**, 155419 (2016).
- [15] M. M. El K. Shehata, G. Simion, R. Li, F. A. Mohiyaddin, D. Wan, M. Mongillo, B. Govoreanu, I. Radu, K. De Greve et al, *Phys. Rev. B* **108**, 045305 (2023).
- [16] J.-Y. Wang, S. Huang, Z. Lei, D. Pan, J. Zhao, and H. Q. Xu, *Appl. Phys. Lett.* **109**, 053106 (2016).
- [17] G. Giavaras, *Physica E* **87**, 129 (2017); *J. Appl. Phys.* **120**, 114301 (2016); *Low Temp. Phys.* **50**, 146 (2024).
- [18] E. Cota, R. Aguado, and G. Platero, *Phys. Rev. Lett.* **94**, 107202 (2005).
- [19] W. Song, T. Du, H. Liu, M. B. Plenio, and J. Cai, *Phys. Rev. Appl.* **12**, 054025 (2019).
- [20] S. J. Chorley, G. Giavaras, J. Wabnig, G. A. C. Jones, C. G. Smith, G. A. D. Briggs, and M. R. Buitelaar, *Phys. Rev. Lett.* **106**, 206801 (2011).
- [21] T. Zhang, H. Liu, F. Gao, G. Xu, K. Wang, X. Zhang, G. Cao, T. Wang, J. Zhang, X. Hu, H.-O. Li, and G.-P. Guo, *Nano Lett.* **21**, 3835 (2021).
- [22] H. Liu, T. Zhang, K. Wang, F. Gao, G. Xu, X. Zhang, S.-X. Li, G. Cao, T. Wang, J. Zhang, X. Hu, H.-O. Li, and G.-P. Guo, *Phys. Rev. Applied* **17**, 044052 (2022).
- [23] G. Giavaras, N. Lambert, and F. Nori, *Phys. Rev. B* **87**, 115416 (2013).
- [24] S. Zhang, Y. He, and P. Huang, *Phys. Rev. B* **107**, 155301 (2023).
- [25] G. Giavaras, J. Wabnig, B. W. Lovett, J. H. Jefferson, and G. A. D. Briggs, *Phys. Rev. B* **82**, 085410 (2010).
- [26] M.-M. Zhang, G.-H. Ding, and B. Dong, *J. Phys.: Condens. Matter* **33**, 475302 (2021).
- [27] K. Ono, S. N. Shevchenko, T. Mori, S. Moriyama, and F. Nori, *Phys. Rev. Lett.* **122**, 207703 (2019).
- [28] G. Giavaras and Y. Tokura, *Phys. Rev. B* **99**, 075412 (2019).
- [29] G. Giavaras and Y. Tokura, *Phys. Rev. B* **100**, 195421 (2019).
- [30] G. Giavaras and Y. Tokura, *J. Appl. Phys.* **128**, 154304 (2020).
- [31] K. Ono, D. G. Austing, Y. Tokura, and S. Tarucha, *Science* **297**, 1313 (2002).
- [32] T. Fujisawa, T. Hayashi, and S. Sasaki, *Rep. Prog. Phys.* **69**, 759 (2006).
- [33] F. Forster, G. Petersen, S. Manus, P. Hänggi, D. Schuh, W. Wegscheider, S. Kohler, and S. Ludwig, *Phys. Rev. Lett.* **112**, 116803 (2014).
- [34] S. N. Shevchenko, A. I. Ryzhov, and F. Nori, *Phys. Rev. B* **98**, 195434 (2018).
- [35] S. N. Shevchenko, S. Ashhab, and F. Nori, *Phys. Rep.* **492**, 1 (2010).
- [36] V. Ivakhnenko, S. N. Shevchenko, and F. Nori, *Phys. Rep.* **995**, 1 (2023).
- [37] S. N.-Perge, V. S. Pribiag, J. W. G. van den Berg, K. Zuo, S. R. Plissard, E. P. A. M. Bakkers, S. M. Frolov, and L. P. Kouwenhoven, *Phys. Rev. Lett.* **108**, 166801 (2012).
- [38] S. Takahashi, R. S. Deacon, K. Yoshida, A. Oiwa, K. Shibata, K. Hirakawa, Y. Tokura, and S. Tarucha, *Phys. Rev. Lett.* **104**, 246801 (2010).
- [39] Y. Kanai, R. S. Deacon, S. Takahashi, A. Oiwa, K. Yoshida, K. Shibata, K. Hirakawa, Y. Tokura, and S. Tarucha, *Nature Nanotechnology* **6**, 511 (2011).
- [40] S. Kohler, J. Lehmann, and P. Hänggi, *Phys. Rep.* **406**, 379 (2005).